Liling_Chemometrics

by

Submission date: 02-May-2023 06:40PM (UTC-0400)
Submission ID: 2082479260
File name: s_applied_to_1H_NMR_and_FTIR_data_for_a_quality_parameter_3.pdf (2.9M)
Word count: 9704
Character count: 49068

Received: 8 September 2022 | Revised: 8 November 2022 | Accepted: 21 November 2022

DOI: 10.1002/pca.3196

RESEARCH ARTICLE

Phytochemical Analysis WILEY

Chemometric analysis applied to ^{1}H NMR and FTIR data for a quality parameter distinction of red fruit (*Pandanus conoideus*, lam.) oil products

Liling Triyasmono[1,2] | Curd Schollmayer[1] | Ulrike Holzgrabe[1]

[1]Institute for Pharmacy and Food Chemistry, University of Würzburg, Würzburg, Germany

[2]Department of Pharmacy, Faculty of Mathematics and Natural Sciences, Lambung Mangkurat University, Banjar Baru, Indonesia

Correspondence
Ulrike Holzgrabe, Institute for Pharmacy and Food Chemistry, University of Würzburg, Am Hubland, 97074 Würzburg, Germany.
Email: ulrike.holzgrabe@uni-wuerzburg.de

Funding information
Lambung Mangkurat University, Grant/Award Number: 3894/UN8/KP/2019

Abstract

Introduction: Red fruit oil (RFO) is a natural product extracted from *Pandanus conoideus* Lam. fruit, a native plant from Papua, Indonesia. Recent studies indicate that RFO is popularly consumed as herbal medicine. Therefore, the quality of RFO must be assured.

Objectives: This study aimed to develop a chemometric analysis applied to ^{1}H nuclear magnetic resonance (NMR) and Fourier transform infrared (FTIR) data for important quality parameter distinction of red fruit oil (RFO), especially regarding the degree of unsaturation and the amount of free fatty acids (FFA).

Materials and methods: Forty samples consisting of one crude RFO, thirty-three commercial RFOs, and three oils as blends, including olive oil, virgin coconut oil, and black seed oil, were analysed by ^{1}H NMR and FTIR spectroscopy. After appropriate preprocessing of the spectra, principal component analysis (PCA) and partial least squares regression (PLSR) were used for model development.

Results: The essential signals for modelling the degree of unsaturation are the signal at $\delta = 5.37–5.27$ ppm (^{1}H NMR) and the band at 3000–3020 cm^{-1} (FTIR). The FFA profile represents the signal at $\delta = 2.37–2.20$ ppm (^{1}H NMR) and the band at 1680–1780 cm^{-1} (FTIR). PCA allows the visualisation grouping on both methods with > 98% total principal component (PC) for the degree of unsaturation and > 88% total PC for FFA values. In addition, the PLSR model provides an acceptable coefficient of determination (R^2) and errors in calibration, prediction, and cross-validation.

Abbreviations: AH, Agro Herbal Husada; AT, Athaku; BMO, Buah Merah oil Papua; BMP, Buah Merah Papua; BMPro, BMPro Minyak Buah Merah; BMW, Buah Merah Wamena; BSO, black seed oil (Habattusauda); CH, Cahaya Minyak Buah Merah; DIO, DioDes Minyak Buah Merah; EZA, Essensa Naturale Buah Merah; FFA, free fatty acid; FR, Fira Herbalindo Buah Merah; GR, golden red; HM, herbal food Buah Merah; HP, Herbal Produk Buah Merah; JW, Jaya Wijaya; KF, KF Minyak Buah Merah; KP, King Pandanus; LJ, Loh Jinawi; MBM, Minyak Buah Merah; MHJ, Mahesa Herbal Jogja; OF, oil fit; OR, crude RFO (original RFO); ORCO, crude RFO plus VCO; ORVO, crude RFO plus olive oil, crude RFO plus black seed oil (Habbatusauda); OVO, olive oil; PCA, principal component analysis; PCI, PCI Buah Merah; PG, premium gold; PI, Papua Indonesia Minyak Buah Merah; PLS, partial least square; PR, Pro Jep Buah Merah; PS, Planta Sehat; PT, Papua Tropika MBM; RD, REDOTEN; RF, Fira Papua; RFO, red fruit oil; RMSEC, root mean square error calibration; RMSEP, root mean square prediction; RMSEV, root mean square error validation; ROP, red oil Papua; RW, Redwin; SBM, Sari Buah Merah Made; TAG, triacylglycerol; THM, Tani Home Industri Buah Merah; TN, Tamba Sanjiwani Natur; VCO, virgin coconut oil.

Conclusion: Chemometric analysis applied to ^{1}H NMR and FTIR spectra of RFO successfully grouped and predicted product quality based on the degree of unsaturation and FFA value categories.

KEYWORDS
^{1}H NMR, degree of unsaturation, FFA value, FTIR, PCA, PLSR, red fruit oil

1 | INTRODUCTION

Red fruit oil (RFO) is a natural product extracted from *Pandanus conoideus* Lam. fruit, a native plant from Papua, Indonesia, and Papua New Guinea. The oval fruits of this tree are some 40–110 cm long, 5–25 cm in diameter, and have a weight of 3–8 kg. This fruit has specific organoleptic properties: red colour with a slightly chelating neutral taste. Traditionally, red fruits are used by Papuans as an edible oil to increase energy and strengthen the immune system. Recent studies have indicated that RFO is popularly consumed as herbal medicine. It is used for medicinal purposes, as the literature records some pharmacological benefits of RFO, such as inhibiting tumour growth and killing cancer cells,[1,2] increasing the number of anti-inflammatory and immune cells,[3] and antioxidant activity.[4] RFO contains active components such as phenols, carotenoids, tocopherols, and unsaturated fatty acids. RFO's reported characteristics differ from other Indonesian vegetable oils, such as coconut and palm oil. RFO contains monounsaturated fatty acid (MUFA) (60%–70%), saturated fatty acid (SFA) (10%–20%), and polyunsaturated acid (PUFA) (2%–10%).[5,6]

The quality of RFO must be assured. One of the oil quality parameters used to assess and classify is the degree of unsaturated lipids and the free fatty acid (FFA) value.[5,7] The conventional method for assessing the degree of unsaturated fatty acids is the determination of the iodine value (IV) and that for quantification of the amount of FFA is the acid value (AV). Unfortunately, the classical IV and AV methods have several drawbacks: they are time-consuming; require sample pretreatment and a large sample size; involve large amounts of organic solvents and harmful chemicals; and lack specificity, which usually depends on a visual endpoint.[8]

To overcome these obstacles, several fast and non-destructive instrumental methods have been proposed for food analysis of the complex mixture, that is, high-resolution techniques such as nuclear magnetic resonance (NMR) and Fourier transform infrared (FTIR) spectroscopy. These methods can provide qualitative and quantitative information in one experiment. The NMR and FTIR spectra, for example, provide information on the product's composition and quality characteristics.[8,9]

For quality assurance purpose, chemometrics is applied directly to the spectral data. These methods are particularly suitable for areas such as food investigations,[10] plant extracts,[11] drug and degradation products,[12,13] and oil authentication and characterisation.[14,15] In the case of successful classification or diagnosis, multiple variables must be considered simultaneously. The use of the Principal Component Analysis (PCA) can accurately visualize the grouping of samples (96%), and the distinction between classes can be sufficient to characterize the geographical origin of oil. The exploratory data analysis mainly consists of PCA, summarising information in large-scale spectrum sets. Another form of data pattern research is partial least squares regression (PLSR), which aims to detect and predict similarities between samples.[16]

The present study aimed to build a model for RFO to guarantee the authenticity of this product using fast and easy-to-automate methodologies, compare different spectroscopic techniques, and investigate whether the synergy among them is able to improve the efficiency of the classification and regression models, especially for the classification of commercial samples of RFO.

2 | EXPERIMENTAL PROCEDURES

2.1 | Materials

Hexa deuterium dimethyl sulfoxide (DMSO-d_6, 99.9% D), tetramethylsilane (TMS), and NMR tube Boro 400-5-7 were purchased from Deutero (Kastellaun, Germany) and deuterated chloroform ($CDCl_3$, 99.8% D) and dimethyl sulfone ($DMSO_2$), internal standard NMR grade, were purchased from Merck (Darmstadt, Germany).

2.2 | All samples

A total of 40 different oils were used in this study, of which 33 samples were commercial RFO products from different factories, purchased from the local traditional herbal market in Jakarta, Indonesia. One crude RFO (OR) sample was obtained from solvent extraction,[17] three samples were OR mixed with other oils, and three different samples, including olive oil (OVO), coconut oil (VCO), and black seed oil (BSO), were the standard oil for additional RFO products (Table 1).The samples were grouped into two categories: calibration and prediction.

For producing model blends, binary mixtures of OVO, VCO, and BSO in OR were prepared by adding BSO, OVO, and VCO to the OR up to a total sample amount of 250.0 mg (1:1.5 w/w), respectively.

2.3 | NMR spectroscopy

A total of 833.33 mg oil and 3.33 mg $DMSO_2$ were weighed into a 2.0-mL reaction tube. After the addition of a solvent mixture of $CDCl_3$

TABLE 1 List of the investigated samples

No	Sample code	Type	Specification	Quantity	Replication number code
1	OR	Crude RFO	Calibration	3	61,62,63
2	ORCO	Crude RFO + VCO	Calibration	3	64.65.66
3	ORVO	Crude RFO + OVO	Calibration	3	67,68,69
4	ORSO	Crude RFO + BSO	Calibration	3	112,113,114
5	OVO	Commercial olive oil	Calibration	3	70,71,72
6	VCO	Commercial virgin coconut oil	Calibration	3	115,116,117
7	BSO	Commercial black seed oil	Calibration	3	118,119,120
8	AT	Commercial	Calibration	3	4,5,6
9	BMO	Commercial	Calibration	3	7,8,9
10	BMP	Commercial	Calibration	3	10,11,12
11	FR	Commercial	Calibration	3	28,29,30
12	GR	Commercial	Calibration	3	31,32,33
13	JW	Commercial	Calibration	3	40,41,42
14	KF	Commercial	Calibration	3	43,44,45
15	KP	Commercial	Calibration	3	46,47,48
16	LJ	Commercial	Calibration	3	49,50,51
17	PG	Commercial	Calibration	3	76,77,78
18	PR	Commercial	Calibration	3	82,83,84
19	RD	Commercial	Calibration	3	91,92,93
20	AH	Commercial	Prediction test	3	1,2,3
21	BMPro	Commercial	Prediction test	3	13,14,15
22	BMW	Commercial	Prediction test	3	16,17,18
23	CH	Commercial	Prediction test	3	19,20,21
24	DIO	Commercial	Prediction test	3	22,23,24
25	EZA	Commercial	Prediction test	3	25,26,27
26	HM	Commercial	Prediction test	3	34,35,36
27	HP	Commercial	Prediction test	3	37,38,39
28	MBM	Commercial	Prediction test	3	52,53,54
29	MHJ	Commercial	Prediction test	3	55,56,57
30	OF	Commercial	Prediction test	3	58,59,60
31	PCI	Commercial	Prediction test	3	73,74,75
32	PI	Commercial	Prediction test	3	79,80,81
33	PS	Commercial	Prediction test	3	85,86,87
34	PT	Commercial	Prediction test	3	88,89,90
35	RF	Commercial	Prediction test	3	94,95,96
36	ROP	Commercial	Prediction test	3	97,98,99
37	RW	Commercial	Prediction test	3	100,101,102
38	SBM	Commercial	Prediction test	3	103,104,105
39	THM	Commercial	Prediction test	3	106,107,108
40	TN	Commercial	Prediction test	3	109,110,111

and DMSO-d_6 (5:1, v/v) containing 0.1% TMS up to 2.0 mL, the tube was closed and vortexed, and 600 μL of this solution was placed into a 5-mm-diameter NMR tube (Boro 400-5-7, Deutero, Kastellaun, Germany). The sample was analysed by NMR spectroscopy (Avance III 400 MHz, Bruker BioSpin GmbH, Rheinstetten, Germany). The experiments were carried out at 300 K; spectral width: 30.0 ppm (time domain size: 160 k), relaxation delay: 9 s, number of scans: 32, acquisition time: 6.81 s, pulse width: 30°, pulse sequence: zg30, no rotation. The receiver gain was set to 4, and a line broadening factor of 0.3 Hz was applied for processing.[18] Previously, measurements of the full

spin–lattice relaxation (T1) of the protons in the sample were carried out according to Holzgrabe[19] and Triyasmono et al[18] The total acquisition time was 15 min.

The spectra were acquired using TopSpin 3.6.4 (Bruker BioSpin GmbH, Rheinstetten, Germany); a manual phase and baseline corrections were applied. All offset signals are referenced to the TMS signal (δ = 0.00 ppm). Each sample was measured in triplicate.

2.4 | FTIR spectroscopy

An FT/IR-6100 spectrometer (JASCO Deutschland GmbH, Pfungstadt, Germany) equipped with an attenuated total reflectance (ATR) unit was used to obtain FTIR spectra. An oil droplet was placed on diamond cell ATR, and the absorbance spectra were recorded. The samples were scanned at room temperature at a resolution of 4 cm^{-1} in a wavenumber range of 4000–600 cm^{-1}. The sample and background spectra were set at an average of over 32 scans. A new background spectrum was obtained after each measurement. The ATR was cleaned with isopropanol before a new sample was applied. All spectra were measured in triplicate and used for statistical analysis.

2.5 | Pre-processing and multivariate data analysis

Data preprocessing of the ^{1}H NMR spectra was carried out using Amix 3.9.15 (Bruker BioSpin GmbH, Rheinstetten, Germany) to reduce by bucketing spectral regions of equal width of 0.009 ppm. After the bucketing spectra were obtained, they were converted into txt format to build the data matrix (Figures S1–S11 in Supplementary Materials 1). The final range used for PCA and PLS was δ = 5.37–5.27 ppm and δ = 2.37–2.20 ppm.

The data preprocessing of FTIR spectra was performed as a baseline correction. Additionally, the scattering effects were removed by means of second-order smoothing polynomials through 25 points (Savitzky–Golay method).[20,21] Finally, the resulting spectra were converted into JCAMP format to build a data matrix. The final FTIR spectral range of interest was limited to 2990–3020 cm^{-1} and 1680–1780 cm^{-1}.

Unscrambler X 11.0 (CAMO Software AS., Oslo, Norway) was used for the individual analysis of both spectral methods using PCA and PLS. First, PCA methods were applied to attain delineated classes according to the degree of unsaturation and FFA value of commercial products. In addition, PLS methods were applied to predict the value of the degree of unsaturation and FFA composition of RFO commercial products.

The unsupervised pattern recognition model PCA and supervised pattern PLS were built on all replicates of all samples, as shown in Table 1. The calibration models were built using nineteen samples (in triplicate), including OR, three modified RFOs, three other oils (BSO, OVO, and VCO), and 15 commercial RFOs. Furthermore, 21 commercial samples (in triplicate) other than those used as calibrations were used to test their class identities. The leave-one-out cross-validation procedure was used to verify the calibration and prediction model. Finally, the total calibration, validation, and prediction errors (RMSEC, RMSEV, and RMSEP) for each model sample were evaluated.[22]

3 | RESULTS AND DISCUSSION

3.1 | Spectral data for multivariate analysis

For multivariate data analysis, it is mandatory to have a sample preparation that generates reproducible spectra. Figure 1 shows the results of bucketing processes demonstrating a good performance for the alignment of RFO ^{1}H NMR spectra.[10,23,24]

Because the ^{1}H NMR spectrum contains several thousand points and is therefore variable, data reduction or clustering is usually used to reduce the dimension of the data. By bucketing, the spectrum is divided into spectral regions, or buckets (also called bins), and the total area in each bucket is calculated to represent the original spectrum. Finally, to make all spectra comparable, the overall sample concentration variation must be taken into account, as was the case with the ^{1}H NMR spectra of the sample. The clustering of spectra of 0.009 ppm bucket gave satisfactory results, especially the reliability of the chemical shift, and the signal intensity was the same as the original spectra for each sample. It is obtained from the sum of the intensities in each set of buckets so that the area under each signal in the spectral region is used instead of the individual intensities.[23,25] As a result, the chemical shift variability around the signal and misalignment could be overcome. Thus, the resulting data matrix variables will slightly vary each iteration for further chemometric analysis processes.

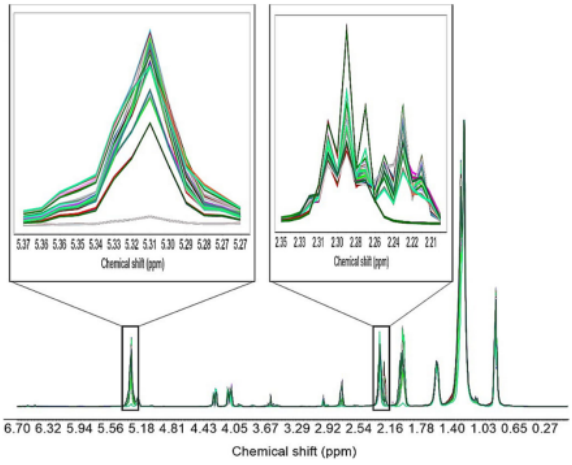

FIGURE 1 Reduced ^{1}H nuclear magnetic resonance (NMR) spectra of all samples with an enlarged spectral range of δ = 5.37–5.27 ppm and δ = 2.37–2.20 ppm. The spectra are colour-coded according to the brand [Colour figure can be viewed at wileyonlinelibrary.com]

Furthermore, in FTIR spectra, preprocessing procedures also showed a good performance for alignment without derivative transformation and data loss with constant range wavenumber. With an interval of 4 cm^{-1} selected, the FTIR spectra sample displays the level of smoothness of the data obtained during the measurement. The meaning of 4 cm^{-1} is that the spectrum is expected to be obtained at intervals of approximately 2 cm^{-1} to increase signal resolution (sharper spectra) without losing time.[26] This result proved that good resolution was obtained between the peak band at 1740 cm^{-1} and 1710 cm^{-1}, as well as at 3007 cm^{-1} and 2920 cm^{-1}, as can be seen in Figure 2. All vibrational bands of sample spectra were obtained clearly at the same wavenumber. Therefore, the resulting data matrix variable will be reliable.

Generally, the spectra produced by these two processing methods have a similar profile in all samples. However, differences in some parts of the intensity on the ^1H NMR and absorbance on the FTIR spectra can be observed, especially in the signals/bands selected for analysis.

Finally, two different matrices were considered for both data:

1. The ^1H NMR matrix consists of two segments: the degree of unsaturation (-C<u>H</u>=C<u>H</u>-) and FFA value (α-CH_2) signals. Thus, the final ^1H NMR data matrix contains 120 rows (samples) and 13 columns for the degree of unsaturation and 120 rows (sample) and 18 columns for FFA values (i.e., relative intensity at different chemical shifts).

2. The FTIR matrix consists of two segments: the degree of unsaturation (the C–H stretching band of the double bond) and FFA value (C=O) bands. Therefore, the final FTIR data matrix contains 120 rows and 33 columns for the degree of unsaturation and 120 rows and 105 columns for FFA values (i.e., absorbance samples at different wavenumbers).

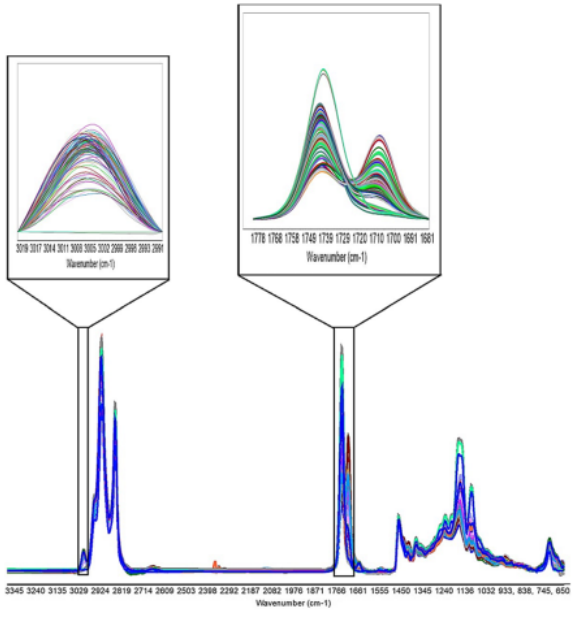

FIGURE 2 Reduced Fourier transform infrared (FTIR) spectra of all samples with an enlarged spectral range of the band at 1780–1680 cm^{-1} and 3020–2990 cm^{-1}. The spectra are colour-coded according to the brand [Colour figure can be viewed at wileyonlinelibrary.com]

3.2 | Evaluation of the correlation-selected signal (-C<u>H</u>=C<u>H</u>-) of the ^1H NMR and FTIR spectra

Both spectral data (^1H NMR and FTIR) consist of triacylglycerol (TAG) and FFA signals which these compound are predominantly found in the intact material analysis.[5,27] The set of signals at δ = 5.37–5.27 ppm arises largely from the ^1H nuclei attached to carbons in the close neighbourhood of a double bond.[28] This signal is related to the degree of unsaturation bonds in a triglyceride, regardless of whether these are located within monounsaturated or polyunsaturated chains. As the FTIR spectra were acquired from precisely the same collection of samples as the one used in the ^1H NMR analysis, an avenue exists for exploring the correlations between the two datasets. In addition, the C–H stretching band of the double bond in the FTIR spectra occurs in the range of 3000–3020 cm^{-1}.[29] Figure 3 displays a multivariate regression showing significant correlations between the ^1H NMR and FTIR dataset points (all PLS model analyses are presented in Figure S1 in Supplementary Materials 2).

The relevant ^1H NMR and FTIR spectral features are -C<u>H</u>=C<u>H</u>-. Even though the FTIR feature has a low intensity, both spectra show relatively strong variations with differences in each product's -C<u>H</u>=C<u>H</u>- bond content. According to Parker et al,[28] these findings can be used as additional information: With a strong correlation between the two spectra, the signal -C<u>H</u>=C<u>H</u>- of NMR and the C-H stretching band of the double bond in the FTIR can be one of the

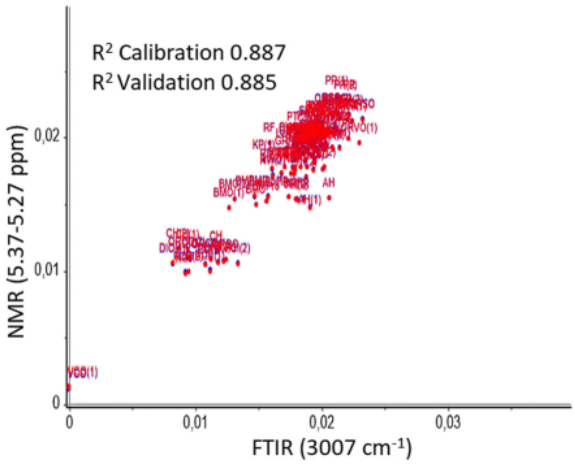

FIGURE 3 Partial least square (PLS) calibration model for the relationship between ^1H nuclear magnetic resonance (NMR) and Fourier transform infrared (FTIR) spectra of the selected signal [Colour figure can be viewed at wileyonlinelibrary.com]

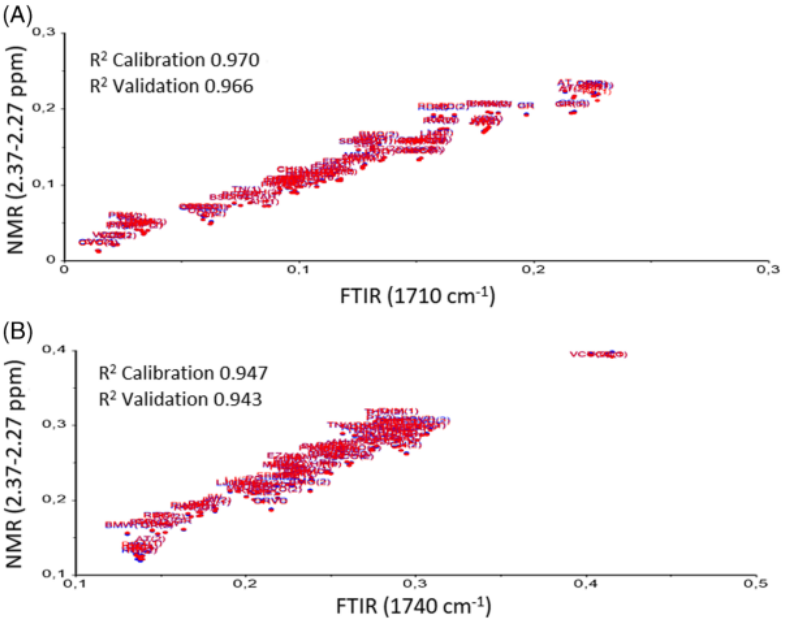

FIGURE 4 Partial least square (PLS) calibration model for the relationship between ^{1}H nuclear magnetic resonance (NMR) and Fourier transform infrared (FTIR) spectra of the selected signal. (A) Band 1710 cm^{-1}; (B) band 1740 cm^{-1} [Colour figure can be viewed at wileyonlinelibrary.com]

signals that determines the difference between the respective oil products, especially regarding the degree of unsaturation.

3.3 | Evaluation of the correlation-selected signal α-CH_2 of the ^{1}H NMR and C=O FTIR spectra

It is well known that C=O at 1710 cm^{-1} can be assigned to -COOH (acid) and C=O at 1740 cm^{-1} to -COOR (ester). The two bands are related to the FFA and TAG system, respectively. Interestingly, a strong correlation can be formed for the α-CH_2 signal of the NMR at δ = 2.37–2.20 ppm and the C=O band resonance of the IR at 1680 to 1780 cm^{-1}. The multivariate regression analysis states that both signals have a closed correlation (R^2 > 0.97 and R^2 > 0.94) (Figure 4; all PLS model analyses are presented in Figure S2 and S3 in Supplementary Materials 2).

However, there are different interpretations of the relationship between the two bands, especially in the OVO, VCO, and OR samples. The C=O band at 1710 cm^{-1}, with a signal α-CH_2 at δ = 2.37–2.20 ppm, indicates that the position of OVO and VCO had the lowest intensity, whereas OR had the highest intensity (Figure 4A). On the other hand, the C=O band at 1740 cm^{-1} indicates that the OVO and VCO have the highest intensity, while OR has the lowest intensity (Figure 4B). These results indicate that the TAG OVO and VCO composition is more significant than FFA. In contrast, OR shows that the composition of FFA is higher than TAG. These results confirm that the C=O band at 1710 cm^{-1} is an acid (FFA), while the C=O band at 1740 cm^{-1} is an ester (TAG).[30]

Parker et al 's[28] have not shown any correlation between the C=O band (FTIR) and the α-CH_2 signal (^{1}H NMR) due to the absence of a heat map in the Pearson correlation statistic. However, our findings indicate strong correlation between the α-CH_2 signal on ^{1}H NMR and the C=O band on FTIR. These results can be obtained because the two signals in each spectrum have good resolution and a relatively substantial intensity difference (see Figure 1 and Figure 2). In addition, these two functional groups are adjacent in the structure of the constituent FFA and TAG.[21,27] Therefore, these two signals/bands are essential in differentiating oil products based on the amount of FFA.

3.4 | Principal component analysis projection for the degree of unsaturation profile distinction

The PCA projection is carried out on the matrix data of the ^{1}H NMR and FTIR spectra related to the degree of unsaturation to predict the RFO product profile. The first PCA was performed on a calibration matrix of 57 spectra from 19 calibration samples. The presence of BSO, OVO, and VCO as a comparison and modifier of OR in calibration modelling illustrates the effect of adding these types of oil to OR in matrix variables (see Section 2). Finally, the PCA calibration results are used to project 63 spectra from 21 samples of RFO products (prediction test). Based on the ability of PCA to determine the similarity between the calibration data model and the prediction data,[31] the RFO samples will be grouped according to the similarity of the variables. They will show the projection pattern due to changes in the variables caused by these modifications, which are also helpful for authentication.

The PCA of ^{1}H NMR data presents the separation of the RFO products into four main regions (Figure 5; all PCA model analyses are displayed in Figure S4 in Supplementary Materials 2). Most RFO products are on the positive side of the PC2 and PC1 axes (red circle),

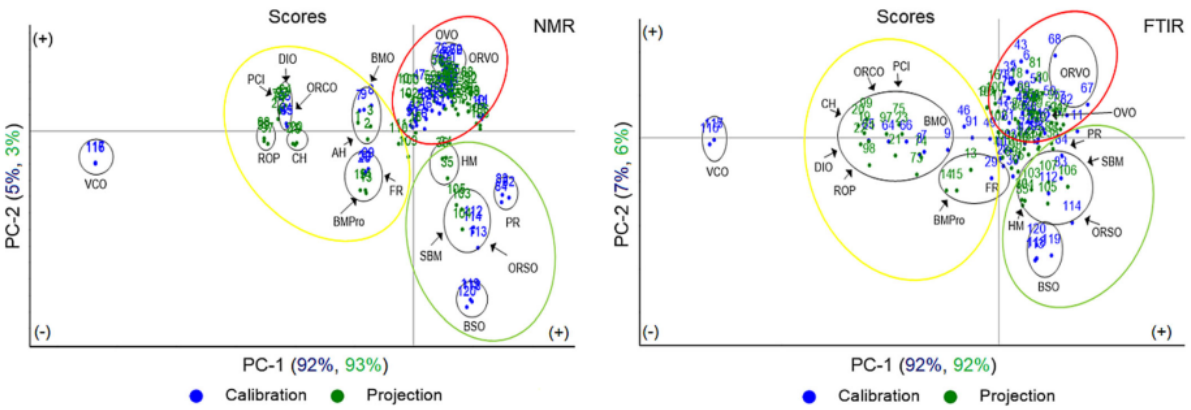

FIGURE 5 Projected twenty-one red fruit oil (RFO) commercial products based on principal components PC1 and PC2 with the selected signal at δ = 5.37–5.27 ppm (-CH=CH-) of the 19 ^{1}H nuclear magnetic resonance (NMR) spectra calibration set (57 spectra) (NMR) and with the selected band at 3000–3020 cm^{-1} (the C–H stretching band of the double bond) of the 19 Fourier transform infrared (FTIR) spectra calibration set (57 samples) (FTIR). The replication number code indicates the label point for each sample (see Section 2). Green circle, ORSO-projected sample group; yellow circle, ORCO-projected sample group; red circle, ORVO-projected sample group. AH, agro herbal Husada; BMO, Buah Merah oil Papua; BMPro, Minyak Buah Merah; BSO, black seed oil; CH, Cahaya; DIO, DioDes Minyak Buah Merah; FR, Fira Papua; ORCO, crude RFO plus VCO; ORSO, crude RFO plus BSO; ORVO, crude RFO plus OVO; PCI, PCI Buah Merah; PR, pro Jep Buah Merah; ROP, red oil Papua; SBM, sari Buah Merah; OVO, olive oil; VCO, virgin coconut oil [Colour figure can be viewed at wileyonlinelibrary.com]

including OVO and ORVO. On the most negative side of the PC1 axis, there are VCO products (outliers/black circle) because it is a type of oil different from RFO (slight/no double bond), while BSO is located at the most negative PC2 (green circle), because of the large number of double bonds. Furthermore, this PCA projection can be used for RFO, delineating classes based on the closeness of the degree of unsaturation category.

Accordingly, PCA calibration and projection plots indicate four products of RFO from the prediction set (ROP, CH, DIO, AH, and BMPro). Three products from the calibration set (ORCO, BMO, and FR) are located in the negative PC1 (yellow circle) that are close to VCO, indicating a profile very similar to the VCO (especially a high amount of saturated lipid). In addition, there are four RFO products in the prediction set, which are similar to one calibration modification product (ORCO). Therefore, these results indicate that the products ROP, CH, DIO, and PCI are estimated to contain VCO.

On the other hand, there are two RFO products of the prediction test (HM and SBM) and two products of the calibration set (PR and ORSO) located on the negative side of the PC2 axis (green circle), where the products are projected close to the BSO profile indicating a lot of double bonds. In addition, there is one RFO product (SBM) in the prediction set, similar to one calibration modification product (ORSO). These results can denote that the product (SBM) is projected to contain BSO. Examination of PC1 and PC2 loading of the ^{1}H NMR data shows that this separation occurs because the spectral domain at δ = 5.37–5.27 ppm (-CH=CH-) has different relative intensities; thus, the signal represents an important limitation of this method.

The treatment of FTIR data appears to have similarities in the projection of the sample product based on the degree of unsaturation. However, in the FTIR in Figure 5, the PCA score plot shows a marked separation in which VCO is located in the most negative PC1 and BSO is in the most negative PC2, while most of the products are found in plots PC1, PC2 are positive (all PCA model analyses are presented in Figure S5 in Supplementary Materials 2). At least, the FTIR PCA plot results are similar to the ^{1}H NMR. Separation of the same products with a close profile to VCO can also be detected. For example, four products of the prediction test (ROP, CH, DIO, and PCI) are projected to ORCO (yellow circle), and the separation of products prediction test (SBM) close to the BSO profile is projected to ORSO (green circle). However, some projected overlapping products and different locations between replications can still be seen. The FTIR data loading assessment of PC1 and PC2 indicated that an absorption band at about 3000–3020 cm^{-1} (the C–H stretching band of the double bond) was responsible for this separation.

Chemometric analysis for both data sets showed projected differences in the degree of unsaturation between the RFO products. The total projection of the two data sets also indicates satisfactory results by producing 98% total principal component (PC) separation into three (yellow, red, and green circles) and VCO regions depending on the degree of unsaturation, as already described. Unfortunately, PCA projections on FTIR show a more considerable grouping variability; for example, the distance differences between product replications of BMPro and PCI in the yellow-circle sample group and of ORSO and PR in the green-circle sample group. The lower reproducibility observed in the FTIR results depends on the manual placement of the sample in the ATR, as has been discussed by Jovic et al.[32] Therefore, the triple-clustering projection for FTIR shows unsatisfactory results. It is important to emphasise that replicate clustering is preferable when ^{1}H NMR is used.

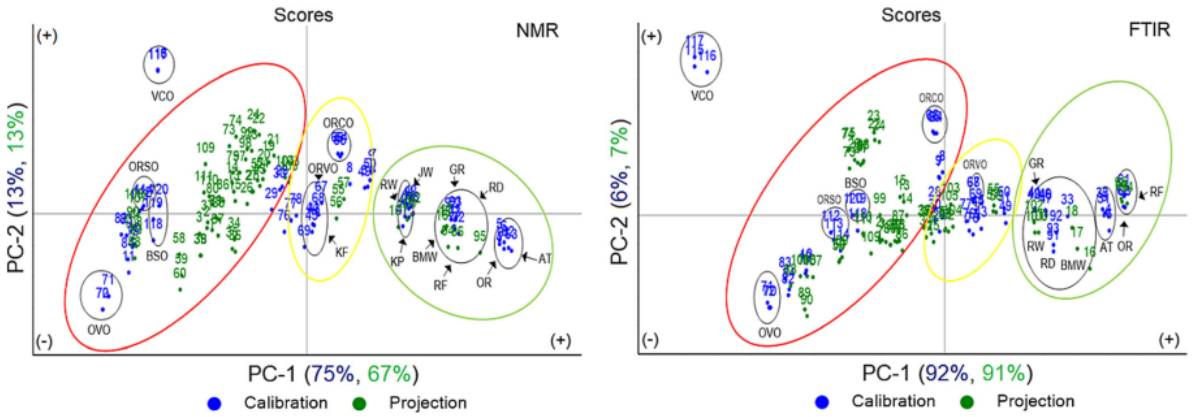

FIGURE 6 Projected 21 red fruit oil (RFO) commercial products based on principal component PC1 and PC2 with the selected signal at δ = 2.37–2.227 ppm (α-CH_2) of the 19 ^{1}H nuclear magnetic resonance (NMR) spectra calibration set (57 spectra) and with the selected band at 1690–1780 cm^{-1} (C=O) of the 19 Fourier transform infrared (FTIR) spectra calibration set (57 spectra). The replication number code indicates the label point for each sample (see Section 2). Green circle, PC-1 positive projected sample group; yellow circle, PC-1 middle projected sample group; red circle, PC-1 negative projected sample group. AT, Athaku; BSO, black seed oil; JW, Jaya Wijaya; KF, KF Minyak Buah Merah; KP, king Pandanus; GR, golden red; OR, crude RFO; ORCO, crude RFO plus VCO; ORVO, crude RFO plus OVO; OVO, olive oil; RD, Redoten; RF, Fira Papua; VCO, virgin coconut oil [Colour figure can be viewed at wileyonlinelibrary.com]

3.5 | Principal component analysis projection for FFA value profile distinction

Principal component analysis projection predicts the RFO product profile based on the FFA value. As mentioned above, the presence of oil other than RFO, including BSO, OVO, and VCO, aims to compare and modify OR to indicate changes in the sample matrix caused by the intervention of each oil. A total of 57 spectra from 19 samples were used as a data calibration matrix for projecting 21 RFO samples (see Section 2). The PCA data for ^{1}H NMR and FTIR present a separation of the RFO products into four regions.

On the other hand, the PCA pattern projection from FTIR shows a pattern similar to NMR (Figure 6; all PCA model analyses are presented in Figures S6 and S7 in Supplementary Materials 2). The 3 RFOs, including OR, AT, and RF (green circle), also lie at the farthest positive PC1, while the PC2 is positive. Meanwhile, most RFO products are projected along PC2 (negative to positive) in the red circle. Another similarity was also shown in the projections of VCO (farthest positive PC2) and OVO (farthest negative PC2) in the red circles.

The modified RFO also has a similar projection to the ^{1}H NMR data. The projected ORSO samples were identical with BSO (PC1 and PC2 were negative) in the red circles. As for the ORCO projection, the FTIR pattern is better than the ^{1}H NMR pattern (PC1 negative and PC2 positive) because it is located in the same quadrant plot as the VCO, while ORSO in the NMR plot score is in the yellow circle. It means that the FTIR spectral pattern for ORCO can show the effect of adding VCO to the variable matrix pattern to be used as a reference for authentication.

Interestingly, the ORVO projections for both PCA patterns also show a similar location at the midpoint of the plot score (PC1 and PC2 are positive) in the yellow circle. However, they are not projected in the same way as OVO (red circle). These results show that the addition of OVO to OR does not necessarily change the pattern of the variable matrix that is close to the OVO pattern. Accordingly, the results illustrate that the difference matrix variables used do not directly affect the projection pattern. This condition depends on the FFA amount of both. Furthermore, the FTIR projection pattern on the selected matrix variable shows a better projection pattern with a full PC of 98%, while ^{1}H NMR can project a full PC of 88%.

3.6 | Principal component analysis for the degree of unsaturation grouping

In the visualisation grouping approach, PCA builds three rules based on the degree of unsaturation content with three different oil products with RFO as standard, namely BSO, OVO, and VCO. When an RFO product has a low degree of unsaturation, it will approach VCO. An RFO product with a high degree of unsaturation identical to OVO is an original RFO product because, based on the characterisation results,[5,6] the main content of RFO is oleic acid. In contrast, an RFO product with a higher degree of unsaturation will approach the BSO position because it has more unsaturated fatty acids than OVO. Furthermore, a visualisation grouping PCA model can be obtained based on the value of the degree of unsaturation for the entire RFO product,[27] as previously reported by Triyasmono et al.[18] Figure 7 shows that both spectral data sets can be delineated classes into six categories (IV: < 10; 40–60; 60–70; 70–80; 80–90; and > 90).

Both ^{1}H NMR and FTIR data presented satisfactory results with 98% total PC and 99% total PC of the classified products, respectively (all PCA model analyses are presented in Figures S8 and S9 in

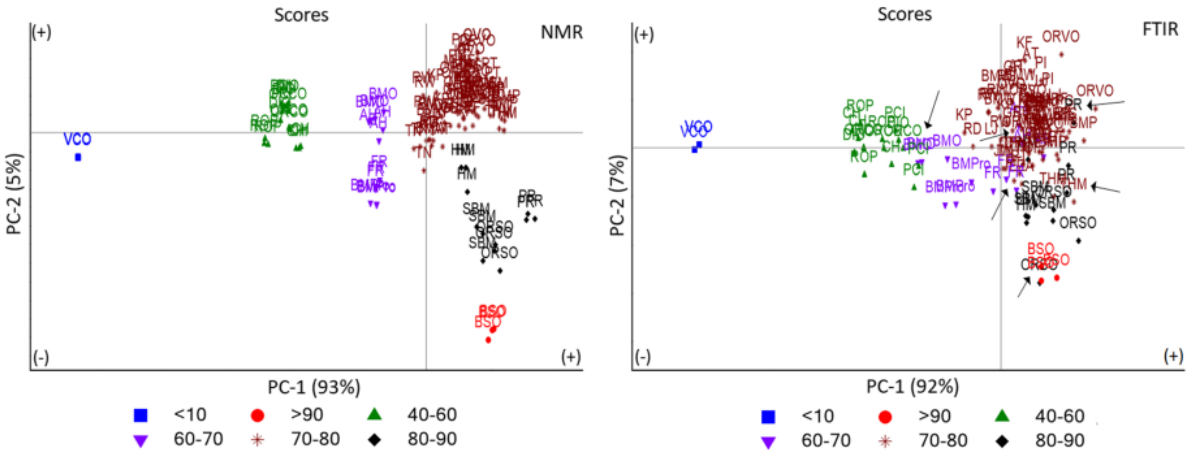

FIGURE 7 Plot scores of all samples (120 spectra) on the main components PC1 and PC2 on the selected signal ^{1}H nuclear magnetic resonance (NMR) spectra and selected band Fourier transform infrared (FTIR) based on the degree of unsaturation category. (point labels are based on the list of abbreviations) [Colour figure can be viewed at wileyonlinelibrary.com]

Supplementary Materials 2). For FTIR data, there are five types of classified products that overlap with the others (AH, BMO, FR, THM, and PR) (Figure 7 FTIR). As for the prediction of ^{1}H NMR, the observations were excellent because 100% of the samples were classified correctly. Furthermore, these results show that most products can be grouped at 70–80 degrees of unsaturation, as well as OVO, which indicates that most RFO products have a MUFA component. On the other hand, four products (ROP, CH, DIO, and PCI) and ORCO are close to VCO, so it is suspected that VCO components were added, causing a decreased degree of unsaturation; therefore, VCO is grouped lower than OR (40–60).

In comparison, three products (SBM, PR, and FR) and ORSO are close to BSO, so it is suspected that BSO was added to the product component, causing an increased degree of unsaturation. Therefore, it is grouped as higher than OR (80–90). Based on the fact there is still miss-grouping in the FTIR data, even though the PCA obtained 99% of total PC can distinguish different variables. Finally, the best triplicate for ^{1}H NMR data implies a perfect visualisation grouping based on the RFO product's unsaturation degree.

3.7 | Principal component analysis for FFA value grouping

Furthermore, for the grouping approach based on its FFA value, the PCA model is based on the acid number possessed by each sample because the amount of FFA depends on the AV of each sample. The FFA in each product occurs either naturally or due to degradation. Meanwhile, the presence of BSO, OVO, and VCO independently and OR modifiers can be used to compare the distribution pattern classification due to changes in the variable matrix (see Section 2). Figure 8 depicts the PCA visualisation grouping of all total samples into seven categories according to acid values based on Triyasmono et al[18] reported (AV: < 10; 20–40; 40–60; 60–70; 70–80, 80–90, and > 90) for the spectrum of both methods.

The PCA plot score generated from both methods (NMR and FTIR) showed the same pattern. However, the ^{1}H NMR data displayed a better classification pattern than the FTIR data because the entire sample could be separated according to their respective categories without overlap (Figure 8; NMR and all PCA model analyses are presented in Figure S10 in Supplementary Materials 2). As for the PCA FTIR data pattern, several sample products are delineated classes into different categories, including AT, CH, DIO, OF, and RF (Figure 8; FTIR and all PCA model analyses are presented in Figure S11 in Supplementary Materials 2). These results were obtained because the FTIR spectrum pattern variance is more significant than ^{1}H NMR so that it can cause a more considerable matrix variable variance.[32] Interestingly, OVO and VCO have the same categorisation of the FFA value at < 10. Both are located on the same PC1 (farthest negative). Meanwhile, they are different in PC2; OVO PC2 is negative while VCO PC2 is positive. These results can be caused by the spectral variance pattern correlated with the chemical bonds of a FFA constituent of each oil. For OVO, FFA mainly consists of oleic acid. Meanwhile, VCO's FFA mostly consists of palmitic acid.[32,33]

In contrast, BSO plot scores mostly differ from RFO products and OVO in the degree of unsaturation category but have adjacent plot scores in the FFA category. This result indicates they may have the same AV even though their FFA composition is different.[9,32,34] Therefore, this signal is suitable for classifying and authenticating commercial RFOs based on the AV profile.

On the other hand, De la Mata et al,[35] employing FTIR and PLS discriminant analysis (PLS-DA) spectra in the entire band at 3508–650 cm^{-1} (except 2350–1870 cm^{-1}), which was derivatised, demonstrated that 100% olive oil was identified and differentiated from vegetable oil. However, up to 50% for mixed samples resulted in a more significant prediction error. In comparison, this finding can also

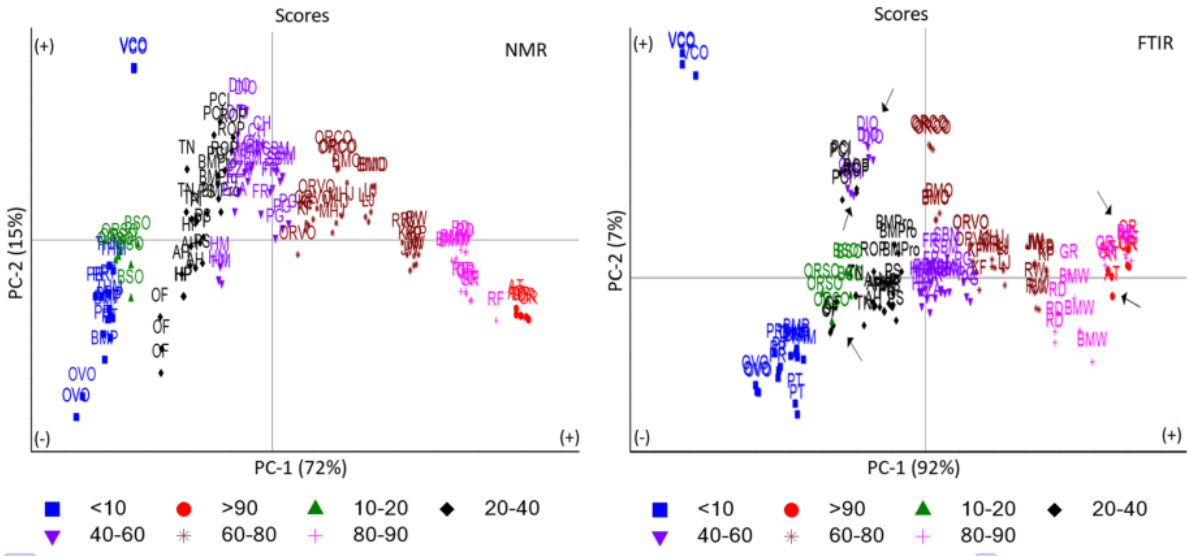

FIGURE 8 Plot scores of all samples (120 spectra) on the main components PC1 and PC2 on the selected signal ^{1}H nuclear magnetic resonance (NMR) spectra and the selected band Fourier transform infrared (FTIR) spectra based on the free fatty acid (FFA) value category. (point labels are based on the list of abbreviations) [Colour figure can be viewed at wileyonlinelibrary.com]

visualise the grouping of the RFO based on the degree of unsaturation and the FFA value up to a total PC of 99% with a lower error prediction even using two bands (3000–3020 cm^{-1} and 1680–1780 cm^{-1}) and without derivatisation spectra.

Popescu et al[36] used NMR spectra (^{1}H, ^{13}C) combined with PCA, and were able to produce projections of olive oil that clustered close together even though they came from different countries of origin, while walnut oil was in varied plots. Subsequently, a mixture of 1% olive oil and sunflower oil could also be detected, with a total PC variance between 91% and 92%. However, the authors could show a total PC variance of up to 98% in visualising the different RFO products and projecting the presence of adulterants, including OVO, BSO, and VCO.

In comparison with the ^{13}C NMR approach without chemometrics for the identification of adulterant vegetable oils in essential oils as described by Truzzi et al,[37] the ^{1}H NMR requires a shorter acquisition time of only 15 min per sample compared with 47 min. One of the reasons for this condition is that the relaxation times of carbon atoms are significantly longer (5.6 s) than those of ^{1}H NMR (1.56 s) in the lipid component.[38,39]

Furthermore, the approach without chemometrics in ^{13}C NMR still entails manually calculating the similarity using the square ratio matrix formula. In comparison, the procedure for chemometrics is relatively simple; the entire bucketing sample spectrum data are directly imported into Unscrambler X 11.0 (see Section 2.5) for PCA and PLS analysis. Therefore, the time needed for analysis was relatively short (approximately 10 min). In addition, by applying chemometrics, groups can be better visualised, with a confidence level of more than 95% and with an acceptable error lower than 5% compared with those without chemometrics: the confidence level obtained was 75%, and the minimum error achieved was 10% in identifying the presence of adulterants in essential oil. Nevertheless, ^{13}C NMR experiments are a worthwhile alternative because they provide significantly more information than the time-consuming determination of, for example, IV.

Finally, the results from this work pointed out that NMR-PCA and FTIR-PCA are suitable and more straightforward as well as quick and efficient methods for describing classes, differentiating RFO types, or detecting adulteration, especially adulteration with other types of oil that have a higher or lower unsaturated degree and FFA values without losing precision.

3.8 | PLS model for prediction of the degree of unsaturation and FFA value

A PLS model is constructed for each parameter (the degree of unsaturation and FFA value). Calibration was performed with leave-one-out cross-validation. Futhermore, model validation was performed by modeling test predictions (see Section 2). Table 2 shows the mean values for each parameter, and the results are presented in terms of the number of factors used, correlation coefficient (R^1), calibration standard error (SEC), and prediction standard error (SEP). SEC and SEP are the standard deviations for the difference between the measured and ^{1}H NMR-estimated values for the samples in the calibration and validation sets, respectively.

The performance results indicate that both parameters show a good match based on the R^2 index with RMSEC for each model lower than SEP.[22] Furthermore, at least 92% of the variation of the output variable can be explained by the ^{1}H NMR and FTIR spectra (all PLS models and predicted analyses are presented in Figures S12-S19 in

TABLE 2 Results of PLS modelling and prediction of the RFO properties based on both methods (^{1}H NMR and FTIR)

Parameter	Method	Value	Factor	R^2			Root mean square error (RMSE)		
				Calibration	Validation	Prediction	RMSEC	RMSEV	RMSEP
Unsaturated degree	^{1}H NMR	0–90	1	0.972	0.967	0.915	3.08	3.29	4.18
	FTIR	0–90	1	0.919	0.914	0.834	5.31	5.49	5.50
FFA value	^{1}H NMR	0–100	2	0.988	0.986	0.982	3.49	3.76	3.12
	FTIR	0–100	2	0.977	0.977	0.948	4.88	5.15	5.10

Abbreviations: FFA, free fatty acid; FTIR, Fourier transform infrared; NMR, nuclear magnetic resonance; RMSEC, root mean square error calibration; RMSEP, root mean square prediction; RMSEV, root mean square error validation.

Supplementary Materials 2). However, ^{1}H NMR data give more results with better reproducibility, indicated by a lower error value for both parameters.

Therefore, ^{1}H NMR replication is more promising and proven to determine the difference between each RFO product based on the degree of unsaturation and the FFA value. These findings support several previous reports[14,15,27,28] on the success of ^{1}H NMR spectroscopy in analysing fat and oil quality parameters.

In conclusion, the spectra profiled by ^{1}H NMR and FTIR followed by chemometric analysis contributed to the discriminant of RFO based explicitly on the degree of unsaturation and the FFA value. Compared with other traditional techniques, ^{1}H NMR and FTIR combined with chemometrics provide a fast and economical method for RFO characterisation, classification, and authentication. Both methods were successful for the projection, grouping, and prediction of the distinction of the degree of unsaturation and FFA value between OR, commercial RFO, and modified RFO. However, better results were achieved for ^{1}H NMR data. These results demonstrate that chemometrics is a robust characterisation, classification, and authentication tool.

ACKNOWLEDGMENTS

The authors would like to thank Lambung Mangkurat University for the supporting finance (Grant No. 3894/UN8/KP/2019). The authors warmly thank Dr. Jens Schmitz, Sebastian Schmidt, and Dr. Alexander Becht for their technical support during the study as well as Dr. Ludwig Höllein for editorial support during writing and preparing for submission this publication. Open Access funding enabled and organized by Projekt DEAL.

FUNDING INFORMATION

This study was financed in part by Lambung Mangkurat University (Grant No. 3894/UN8/KP/2019), Indonesia and the Institute for Pharmacy and Food Chemistry, Wuerzburg University, Germany.

ETHICS STATEMENT

Our research did not include any human subjects or animal experiments.

DATA AVAILABILITY STATEMENT

The data that support the findings of this study are available in the supplementary material of this article.

ORCID

Ulrike Holzgrabe https://orcid.org/0000-0002-0364-7278

REFERENCES

1. Mun'im A, Andrajati R, Susilowati H. Tumorigenesis inhibition of water extract of red fruit (*Pandanus conoideus* lam.) on Sprague–Dawley rat female induced by 7,12-dimetilbenz(a)antrasen (DMBA). *Indon J Pharm Sci*. 2006;3:153-161. doi:10.7454/psr.v3i3.3407
2. Surono I, Endaryanto TA, Nishigaki T. Indonesian biodiversities from microbes to herbal plants as potential functional foods. *J Fac Agric Shinshu Univ*. 2008;44(1.2):23-27.
3. Khiong K, Adhika OA, Chakravitha M. Inhibition of NF-κB pathway as the therapeutic potential of red fruit (Pandanus conoideus lam.) in the treatment of inflammatory bowel disease. *JKM (Jurnal Kedokteran Maranatha)*. 2009;9(1):69-75.
4. Rohman A, Riyanto S, Yuniarti N, Saputra WR, Utami R, Mulatsih W. Antioxidant activity, total phenolic, total flavanoid of extracts and fractions of red fruit (Pandanus conoideus lam). *Int Food Res J*. 2010; 17:97-106.
5. Rohman A, Sugeng R, Che Man YB. Characterizaton of red fruit (Pandanus conoideus lam) oil. *Int Food Res J*. 2012;19(2):563-567.
6. Sarungallo ZL, Hariyadi P, Andarwulan N, Purnomo EH. Characterization of chemical properties, lipid profile, total phenol and tocopherol content of oils extracted from nine clones of red fruit (Pandanus conoideus). *J Natural Sci*. 2015;49(2):237-250.
7. Triyasmono L, Riyanto S, Rohman A. Determination of iodine value and acid value of red fruit oil by infrared spectroscopy and multivariate calibration. *Int Food Res J*. 2013;20(6):3259-3263.
8. Ropodi AI, Panagou EZ, Nychas GJE. Data mining derived from food analyses using non-invasive/non-destructive analytical techniques; determination of food authenticity, quality & safety in tandem with computer science disciplines. *Trends Food Sci Technol*. 2016;50:11-25. doi:10.1016/j.tifs.2016.01.011
9. Rohman A, Ghazali MAB, Windarsih A, Irnawati RS, Yusof FM, Mustafa S. Comprehensive review on application of FTIR spectroscopy coupled with Chemometrics for authentication analysis of fats and oils in the food products. *Molecules*. 2020;25(22):5485. doi:10.3390/molecules25225485
10. Monakhova YB, Kuballa T, Lachenmeier DW. Chemometric methods in NMR spectroscopic analysis of food products. *J Anal Chem*. 2013; 68(9):755-766. doi:10.1134/S1061934813090098
11. Alcantara GB, Honda NK, Ferreira MM, Ferreira AG. Chemometric analysis applied in 1H HR-MAS NMR and FT-IR data for chemotaxonomic distinction of intact lichen samples. *Anal Chim Acta*. 2007; 595(1-2):3-8. doi:10.1016/j.aca.2007.03.032
12. Becht A, Schollmayer C, Monakhova YB, Holzgrabe U. Tracing the origin of paracetamol tablets by near-infrared, mid-infrared, and nuclear magnetic resonance spectroscopy using principal component analysis and linear discriminant analysis. *Anal Bioanal Chem*. 2021; 413(11):3107-3118. doi:10.1007/s00216-021-03249-z

13. Roberto de Alvarenga Junior B, Lajarim Carneiro R. Chemometrics approaches in forced degradation studies of pharmaceutical drugs. *Molecules*. 2019;24(3804):1-24 *(Basel, Switzerland)*. NLM (Medline). doi:10.3390/molecules24203804
14. Ingallina C, Cerreto A, Mannina L, et al. Extra-virgin olive oils from nine italian regions: An ^{1}H NMR-chemometric characterization. *Metabolites*. 2019;9(4):1-12. doi:10.3390/metabo9040065
15. Giese E, Rohn S, Fritsche J. Chemometric tools for the authentication of cod liver oil based on nuclear magnetic resonance and infrared spectroscopy data. *Anal Bioanal Chem*. 2019;411(26):6931-6942. doi:10.1007/s00216-019-02063-y
16. Rodionova OY, Pomerantsev AL. Chemometrics: achievements and prospects. *Russ Chem Rev*. 2006;75(4):271-287. doi:10.1070/rc2006v075n04abeh003599
17. Folch J, Lees M, Sloane Stanley GH. A simple method for the isolation and purification of total lipides from animal tissues. *J Biol Chem*. 1957;226(1):497-509. doi:10.1016/s0021-9258(18)64849-5
18. Triyasmono L, Schollmayer C, Schmitz J, et al. Simultaneous determination of the saponification value, acid value, Ester value, and iodine value in commercially available red fruit oil (Pandanus conoideus, lam.) using ^{1}H qNMR spectroscopy. *Food Anal Methods*. 2022;1-13. doi:10.1007/s12161-022-02401-4
19. Holzgrabe U. Quantitative NMR spectroscopy in pharmaceutical applications. *Prog Nucl Magn Reson Spectrosc*. 2010;57(2):229-240. doi:10.1016/j.pnmrs.2010.05.001
20. Savitzky A, Golay MJE. Smoothing and differentiation of data by simplified least squares procedures. *Anal Chem*. 1964;36(8):1627-1639. doi:10.1021/ac60214a047
21. Casale M, Oliveri P, Casolino C, et al. Characterisation of PDO olive oil chianti Classico by non-selective (UV-visible, NIR and MIR spectroscopy) and selective (fatty acid composition) analytical techniques. *Anal Chim Acta*. 2012;712:56-63. doi:10.1016/j.aca.2011.11.015
22. Schönberger T, Monakhova YB, Lachenmeier DW, Walch S, Kuballa T, (NEXT) -NMR working group. EUROLAB Technical Report 01/2015. Guide to NMR Method Development and Validation-Part II: Multivariate data analysis. 2016; (01):1–20. 10.13140/RG.2.1.4265.1289
23. Sousa SAA, Magalhães A, Ferreira MMC. Optimized bucketing for NMR spectra: three case studies. *Chemom Intel Lab Syst*. 2013;122:93-102. doi:10.1016/j.chemolab.2013.01.006
24. Vu TN, Valkenborg D, Smets K, et al. An integrated workflow for robust alignment and simplified quantitative analysis of NMR spectrometry data. *BMC Bioinform*. 2011;12(405):1-14. doi:10.1186/1471-2105-12-405
25. Jellema RH, Brown SD, Tauler R, Walczak B. Comprehensive Chemometrics in: Variable shift and alignment. In: *Chemical and biochemical data analysis*. Vol.2. Oxford: Elsevier; 2009:85-108. doi:10.1016/B978-044452701-1.00104-6
26. Gulmine JV, Janissek PR, Heise HM, Akcelrud L. Polyethylene characterization by FTIR. *Polym Test*. 2002;21(5):557-563. doi:10.1016/S0142-9418(01)00124-6
27. Guillén MD, Ruiz A. Rapid simultaneous determination by proton NMR of unsaturation and composition of acyl groups in vegetable oils. *Eur J Lipid Sci Technol*. 2003;105(11):688-696. doi:10.1002/ejlt.200300866
28. Parker T, Limer E, Watson AD, Defernez M, Williamson D, Kemsley EK. 60 MHz ^{1}HNMR spectroscopy for the analysis of edible oils. *TrAC - Trends Anal Chem*. 2014;57(100):147-158. doi:10.1016/j.trac.2014.02.006
29. An Z, Jiang X, Xiang G, Fan L, He L, Zhao W. A simple and practical method for determining iodine values of oils and fats by the FTIR spectrometer with an infrared quartz Cuvette. *Anal Methods*. 2017;9(24):3669-3674. doi:10.1039/C7AY00727B
30. Lievens C, Mourant D, He M, Gunawan R, Li X, Li CZ. An FT-IR spectroscopic study of carbonyl functionalities in bio-oils. *Fuel*. 2011;90(11):3417-3423. doi:10.1016/j.fuel.2011.06.001
31. Wold S, Esbensen K, Geladi P. Principal component analysis. *Chemom Intel Lab Syst*. 1987;2(1–3):37-52p. doi:10.1007/978-0-387-87811-9_2
32. Jović O, Smolić T, Primožič I, Hrenar T. Spectroscopic and Chemometric analysis of binary and ternary edible oil mixtures: qualitative and quantitative study. *Anal Chem*. 2016;88(8):4516-4524. doi:10.1021/acs.analchem.6b00505
33. Rohman A, Irnawati, Erwanto Y, et al. Virgin coconut oil: extraction, physicochemical properties, biological activities and its authentication analysis. *Food Rev Int*. 2021;37(1):46-66. doi:10.1080/87559129.2019.1687515
34. Lutterodt H, Luther M, Slavin M, et al. Fatty acid profile, thymoquinone content, oxidative stability, and antioxidant properties of cold-pressed black cumin seed oils. *LWT - Food Sci and Technology*. 2010;43(9):1409-1413. doi:10.1016/j.lwt.2010.04.009
35. De la Mata P, Dominguez-Vidal A, Bosque-Sendra JM, Ruiz-Medina A, Cuadros-Rodríguez L, Ayora-Cañada MJ. Olive oil assessment in edible oil blends by means of ATR-FTIR and chemometrics. *Food Control*. 2012;23(2):449-455. doi:10.1016/j.foodcont.2011.08.013
36. Popescu R, Costinel D, Dinca OR, Marinescu A, Stefanescu I, Ionete RE. Discrimination of vegetable oils using NMR spectroscopy and chemometrics. *Food Control*. 2015;48:84-90. doi:10.1016/j.foodcont.2014.04.046
37. Truzzi E, Marchetti L, Benvenuti S, Ferroni A, Rossi MC, Bertelli D. Novel strategy for the recognition of adulterant vegetable oils in essential oils commonly used in food industries by applying 13C NMR spectroscopy. *J Agric Food Chem*. 2021;69(29):8276-8286. doi:10.1021/acs.jafc.1c02279
38. Vlahov G. Application of NMR to the study of olive oils. *Prog Nucl Magn Reson Spectrosc*. 1999;35(4):341-357. doi:10.1016/S0079-6565(99)00015-1
39. Alexandri E, Ahmed R, Siddiqui H, Choudhary MI, Tsiafoulis CG, Gerothanassis IP. High resolution NMR spectroscopy as a structural and analytical tool for unsaturated lipids in solution. *Molecules*. 2017;22(10):1-71. doi:10.3390/molecules22101663

SUPPORTING INFORMATION

Additional supporting information can be found online in the Supporting Information section at the end of this article.

How to cite this article: Triyasmono L, Schollmayer C, Holzgrabe U. Chemometric analysis applied to ^{1}H NMR and FTIR data for a quality parameter distinction of red fruit (*Pandanus conoideus*, lam.) oil products. *Phytochemical Analysis*. 2022;1-12. doi:10.1002/pca.3196

Liling_Chemometrics

ORIGINALITY REPORT

17%	8%	14%	%
SIMILARITY INDEX	INTERNET SOURCES	PUBLICATIONS	STUDENT PAPERS

PRIMARY SOURCES

1	Casale, M.. "Characterisation of PDO olive oil Chianti Classico by non-selective (UV-visible, NIR and MIR spectroscopy) and selective (fatty acid composition) analytical techniques", Analytica Chimica Acta, 20120127 Publication	1%
2	Editha Giese, Ole Winkelmann, Sascha Rohn, Jan Fritsche. "Determining quality parameters of fish oils by means of 1 H nuclear magnetic resonance, mid-infrared, and near-infrared spectroscopy in combination with multivariate statistics", Food Research International, 2018 Publication	1%
3	www.mdpi.com Internet Source	1%
4	Masili, Alice, Sonia Puligheddu, Lorenzo Sassu, Paola Scano, and Adolfo Lai. "Prediction of physical-chemical properties of crude oils by ^{1}H NMR analysis of neat samples and chemometrics : Prediction of physical-chemical properties of crude oils by NMR and	1%

chemometrics", Magnetic Resonance in Chemistry, 2012.
Publication

5	Glaucia Braz Alcantara, Neli Kika Honda, Márcia Miguel Castro Ferreira, Antonio Gilberto Ferreira. "Chemometric analysis applied in 1H HR-MAS NMR and FT-IR data for chemotaxonomic distinction of intact lichen samples", Analytica Chimica Acta, 2007 Publication	1 %
6	www.inrialpes.fr Internet Source	1 %
7	Mujahid Amin, Shahzad Sharif, Sumia Akram, Gulzar Muhammad, Saqib Amin, Rizwan Ashraf, Muhammad Mushtaq. "A dispersive liquid–liquid microextraction followed by reverse - phase high - performance liquid chromatography for QuEChERS determination of chlorogenic acid", Phytochemical Analysis, 2022 Publication	1 %
8	Catherine Deborde, Jean-Xavier Fontaine, Daniel Jacob, Adolfo Botana et al. "Optimizing 1D 1H-NMR profiling of plant samples for high throughput analysis: extract preparation, standardization, automation and spectra processing", Metabolomics, 2019 Publication	<1 %

9	Maria Enrica Di Pietro, Alberto Mannu, Andrea Mele. "NMR Determination of Free Fatty Acids in Vegetable Oils", Processes, 2020 Publication	<1 %
10	Optical Spectroscopy and Computational Methods in Biology and Medicine, 2014. Publication	<1 %
11	Giese, Editha, Ole Winkelmann, Sascha Rohn, and Jan Fritsche. "Towards determining fat quality parameters of fish oil by means of 1 H NMR spectroscopy : 1 H NMR spectroscopy to determine fish oil quality", European Journal of Lipid Science and Technology, 2016. Publication	<1 %
12	researchsystem.canberra.edu.au Internet Source	<1 %
13	enbis.org Internet Source	<1 %
14	T. Parker, E. Limer, A.D. Watson, M. Defernez, D. Williamson, E. Kate Kemsley. "60MHz 1H NMR spectroscopy for the analysis of edible oils", TrAC Trends in Analytical Chemistry, 2014 Publication	<1 %
15	ur.booksc.me Internet Source	<1 %

16	Eleonora Truzzi, Lucia Marchetti, Stefania Benvenuti, Annalisa Ferroni, Maria Cecilia Rossi, Davide Bertelli. " Novel Strategy for the Recognition of Adulterant Vegetable Oils in Essential Oils Commonly Used in Food Industries by Applying C NMR Spectroscopy ", Journal of Agricultural and Food Chemistry, 2021 Publication	<1 %
17	ifrj.upm.edu.my Internet Source	<1 %
18	Jakes, W., A. Gerdova, M. Defernez, A.D. Watson, C. McCallum, E. Limer, I.J. Colquhoun, D.C. Williamson, and E.K. Kemsley. "Authentication of beef versus horse meat using 60MHz 1H NMR spectroscopy", Food Chemistry, 2015. Publication	<1 %
19	Markus Zilker, Fritz Sörgel, Ulrike Holzgrabe. "A long - time stability study of 50 drug substances representing common drug classes of pharmaceutical use", Drug Testing and Analysis, 2019 Publication	<1 %
20	Jonas Wohlfart, Ulrike Holzgrabe. "Analysis of histamine and sisomicin in gentamicin: Search for the causative agents of adverse effects", Archiv der Pharmazie, 2021	<1 %

Publication

21	Mariana-Atena Poiana, Ersilia Alexa, Melania-Florina Munteanu, Ramona Gligor, Diana Moigradean, Constantin Mateescu. "Use of ATR-FTIR spectroscopy to detect the changes in extra virgin olive oil by adulteration with soybean oil and high temperature heat treatment", Open Chemistry, 2015 Publication	<1 %
22	Abdul Rohman, Yaakob B. Che Man, Sugeng Riyanto. "Authentication Analysis of Red Fruit (Pandanus Conoideus Lam) Oil Using FTIR Spectroscopy in Combination with Chemometrics", Phytochemical Analysis, 2011 Publication	<1 %
23	Abdul Rohman, Yaakob B. Che Man. "Analysis of Cod-Liver Oil Adulteration Using Fourier Transform Infrared (FTIR) Spectroscopy", Journal of the American Oil Chemists' Society, 2009 Publication	<1 %
24	www.arxiv-vanity.com Internet Source	<1 %
25	Endah Prasetia Susanti, Abdul Rohman, Widiastuti Setyaningsih. "Dual Response Optimization of Ultrasound-Assisted Oil Extraction from Red Fruit (Pandanus	<1 %

conoideus): Recovery and Total Phenolic Compounds", Agronomy, 2022
Publication

26	Leilei Yu, Zhen Yu, Lijuan Yang, Shibao Wen, Zhen Xiu Zhang. "Development of thermoplastic polyether ester elastomer microcellular foam with high resilience: Effect of chain extension on foaming behavior and mechanical properties", Journal of Applied Polymer Science, 2023 Publication	<1 %
27	www.thaiscience.info Internet Source	<1 %
28	Jan Schripsema, Ronald dos Santos Merlim, Lais Gonçalves Parvan, Helen Sant'Ana dos Santos Ribeiro et al. "Towards a holistic view of tablet quality, an extensive study on paracetamol tablets with nuclear magnetic resonance using similarity calculations, differential NMR and hierarchical cluster analysis", Journal of Pharmaceutical and Biomedical Analysis, 2022 Publication	<1 %
29	hal.archives-ouvertes.fr Internet Source	<1 %
30	Abdul Rohman, Yaakob B. Che Man, Amin Ismail, Puziah Hashim. "Application of FTIR Spectroscopy for the Determination of Virgin	<1 %

	Coconut Oil in Binary Mixtures with Olive Oil and Palm Oil", Journal of the American Oil Chemists' Society, 2010 Publication	
31	biblioteca.puntoedu.edu.ar Internet Source	<1 %
32	kupdf.net Internet Source	<1 %
33	www.sweetstudy.com Internet Source	<1 %
34	Boffo, E.F.. "Classification of Brazilian vinegars according to their ^1H NMR spectra by pattern recognition analysis", LWT - Food Science and Technology, 200911 Publication	<1 %
35	Guillen, M.D.. "Study by means of ^1H nuclear magnetic resonance of the oxidation process undergone by edible oils of different natures submitted to microwave action", Food Chemistry, 200606 Publication	<1 %
36	haemophilia.org.uk Internet Source	<1 %
37	mdpi.com Internet Source	<1 %
38	www4.di.uminho.pt Internet Source	

		<1%
39	www.science.gov Internet Source	<1%
40	bmcinfectdis.biomedcentral.com Internet Source	<1%
41	repository.javeriana.edu.co Internet Source	<1%
42	Adrian J. Charlton, William H. H. Farrington, Paul Brereton. " Application of H NMR and Multivariate Statistics for Screening Complex Mixtures: Quality Control and Authenticity of Instant Coffee ", Journal of Agricultural and Food Chemistry, 2002 Publication	<1%
43	Deisy dos Santos Freitas, Glaucia Braz Alcantara. " Metabolic Study of Dioecy in : NMR-based and Chemometric Approaches ", Phytochemical Analysis, 2018 Publication	<1%
44	Laura Del Coco, Serena Felline, Chiara Girelli, Federica Angilè et al. "1H NMR Spectroscopy and MVA to Evaluate the Effects of Caulerpin-Based Diet on Diplodus sargus Lipid Profiles", Marine Drugs, 2018 Publication	<1%

45	classroomclipart.com Internet Source	<1 %
46	peerj.com Internet Source	<1 %
47	serdp-estcp.org Internet Source	<1 %
48	www.breastcancerupdate.com Internet Source	<1 %
49	Aadil Bajoub, Alessandra Bendini, Alberto Fernández-Gutiérrez, Alegría Carrasco-Pancorbo. "Olive oil authentication: A comparative analysis of regulatory frameworks with especial emphasis on quality and authenticity indices, and recent analytical techniques developed for their assessment. A review", Critical Reviews in Food Science and Nutrition, 2017 Publication	<1 %
50	Alec Sevilla, Jérémy Chéret, Wendy Lee, Ralf Paus. "Concentration ‐ dependent stimulation of melanin production as well as melanocyte and keratinocyte proliferation by melatonin in human eyelid epidermis", Experimental Dermatology, 2023 Publication	<1 %

51	Aziz Hirri, Mahfould Bassbasi, Stefan Platikanov, Roma Tauler, Abdelkhalek Oussama. "FTIR Spectroscopy and PLS-DA Classification and Prediction of Four Commercial Grade Virgin Olive Oils from Morocco", Food Analytical Methods, 2015 Publication	<1 %
52	Brescia, Maria Antonietta, Giuliano Di Martino, Clara Fares, Natale Di Fonzo, Cristiano Platani, Stefano Ghelli, Fabiano Reniero, and Antonio Sacco. "Characterization of Italian Durum Wheat Semolina by Means of Chemical Analytical and Spectroscopic Determinations", Cereal Chemistry, 2002. Publication	<1 %
53	Encarnación Goicoechea, María D. Guillen. " Analysis of Hydroperoxides, Aldehydes and Epoxides by H Nuclear Magnetic Resonance in Sunflower Oil Oxidized at 70 and 100 °C ", Journal of Agricultural and Food Chemistry, 2010 Publication	<1 %
54	Sara Erasmus, Saskia van Ruth. "Key challenges and developments in non-targeted methods or systems to identify food adulteration", Burleigh Dodds Science Publishing Limited, 2021 Publication	<1 %

55	Silvana Nisgoski, Felipe Zatt Schardosin, Francielli Rodrigues Ribeiro Batista, Graciela Inés Bolzon de Muñiz et al. "Potential use of NIR spectroscopy to identify Cryptomeria japonica varieties from southern Brazil", Wood Science and Technology, 2015 Publication	<1 %
56	documents.worldbank.org Internet Source	<1 %
57	fr.scribd.com Internet Source	<1 %
58	upcommons.upc.edu Internet Source	<1 %
59	Ş.C. Bölükbaşi. "Effect of dietary conjugated linoleic acid (CLA) on broiler performance, serum lipoprotein content, muscle fatty acid composition and meat quality during refrigerated storage", British Poultry Science, 2006 Publication	<1 %
60	Anton Gradišek, Mario Cifelli, Donatella Ancora, Ana Sepe, Boštjan Zalar, Tomaž Apih, Valentina Domenici. "Analysis of Extra Virgin Olive Oils from Two Italian Regions by Means of Proton Nuclear Magnetic Resonance Relaxation and Relaxometry Measurements",	<1 %

Journal of Agricultural and Food Chemistry, 2021
Publication

61 Sanoop Pulassery, Bini Abraham, Nandu Ajikumar, Arun Munnilath, Karuvath Yoosaf. "Rapid Iodine Value Estimation Using a Handheld Raman Spectrometer for On-Site, Reagent-Free Authentication of Edible Oils", ACS Omega, 2022 <1%
Publication

62 Jack T. W. E. Vogels, Loes Terwel, Albert C. Tas, Frans van den Berg, Fred Dukel, Jan van der Greef. "Detection of Adulteration in Orange Juices by a New Screening Method Using Proton NMR Spectroscopy in Combination with Pattern Recognition Techniques", Journal of Agricultural and Food Chemistry, 1996 <1%
Publication

Exclude quotes	On	Exclude matches	Off
Exclude bibliography	On		